Universidad de Valladolid

FACULTAD DE CIENCIAS

TRABAJO FIN DE MÁSTER

Máster en Nanociencia y Nanotecnología Molecular

Study of the effects of different polymerization methods on open-cell microcellular materials based on PMMA gelled with acetone.

Mario Fernández de la Fuente
Judith Martín de León y Miguel Ángel Rodríguez Pérez

2022-2023

AGRADECIMIENTOS:

En primer lugar, quiero dar las gracias a Miguel Ángel Rodríguez Pérez por la oportunidad de realizar este trabajo en el laboratorio de CellMat. Un sitio lleno de buena gente y buenos profesionales.

En especial a todxs lxs compañerxs que día a día han hecho de los descanso, los cafés y los ensayos algo divertido. Son lo que en días difíciles en laboratorio me sacan una sonrisa.

En segundo lugar, a mi tutora y compañera de laboratorio Judith Martín. Sin ella nada de esto habría sido posible. Por confiar en mí, aunque a veces yo no lo haga; y por dedicarme tiempo. Por enseñarme día a día a ser mejor investigador.

Gracias a todas las personas que me han acompañado fuera del ambiente científico. Desde mis amigxs hasta mi familia, apoyo indispensable durante toda mi vida.

Finalmente, a una persona muy especial que la vida ha puesto en mi camino para que esta sea más bonita y fácil. Te quiero África.

ÍNDICE:

RESUMEN:

Los polímeros microcelulares se caracterizan por tener tamaños de celdas en el rango de decenas a cientos de micrómetros y densidades de nucleación superiores a 10^9 nucleos/cm^3. Estos materiales han despertado gran interés en el campo de la Ciencia de Materiales debido a sus propiedades interesantes, como una conductividad térmica reducida y buenas propiedades mecánicas. Para otras aplicaciones; como membranas o filtros, las celdas necesitan estar conectadas entre sí. El control de la estructura de estos materiales es muy útil para este tipo de aplicaciones.

Este trabajo se centra en la producción de materiales celulares mediante la expansión de un gel a base de PMMA utilizando acetona como disolvente y un proceso de espumado por disolución de gas con CO_2 supercrítico. Estos diferentes PMMA se han polimerizado específicamente para este trabajo mediante diferentes métodos (Suspensión, Emulsión, Masa y Dispersión). Los parámetros de temperatura de espumado (55ºC), presión de saturación (250 bar) y tiempo de saturación (1 hora) se han mantenido constantes durante todo el trabajo.

Se han fabricado cinco de estos materiales espumados (Suspensión, Suspensión_1, Emulsión, Masa_0.04, Masa_0.3 y Dispersión) y uno comercial (V825T) con diferentes pesos moleculares y polidispersidades para posteriormente caracterizarlos. Con las imágenes obtenidas mediante microscopía electrónica (SEM) y la herramienta de análisis de imágenes ImageJ/FIJI, se ha medido la densidad relativa, el tamaño promedio de las células, la densidad de nucleación y la homogeneidad en sus estructuras.

Los materiales sólidos de PMMA tienen un rango de 964.500 a 63.750 g/mol para el peso molecular, de 6.4 a 1.5 para la polidispersidades, de 1.19 g/cm^3 para la densidad y de 114.57 a 126.29 ºC para la temperatura de transición vítrea.

Los materiales celulares fabricados presentan una amplia variedad en sus estructuras internas. Estas abarcan densidades relativas entre 0.15 y 0.52, tamaños promedio de celda entre 1.2 y 73.9 µm y densidades de nucleación entre $2.9 \cdot 10^7$ - $2.9 \cdot 10^{11}$ celdas/cm^3. Se ha verificado que todos ellos dependen de los parámetros de fabricación.

ABSTRACT:

Microcellular polymers are characterised by cell sizes in the range of tens to hundreds of micrometres and cell nucleation densities higher than 10^9nuclei/cm^3. These materials have aroused great interest in Materials Science area due to their interesting properties, such as a reduced thermal conductivity and good mechanical properties in comparison to conventional cellular polymers (with cells above hundreds of microns). One interesting application for such materials is their use as membranes or filters due to its high specific surface and small pores. For these applications it is mandatory for the cells need to be connected one with each other's.

Microcellular polymers are usually produced through gas dissolutions foaming, however control the open cell content while tailoring the cellular structure is not an easy task.

This work focuses on the production of cellular materials by expanding a PMMA-based gel, using acetone as solvent and dissolution gas foaming process with super critical CO_2. This PMMA has been polymerized specifically for this subject by different methods (Suspension, Emulsion, Bulk and Dispersion). The parameters of foaming temperature (55ºC), saturation pressure (250 bar) and saturation time (1 hour) have been kept constant throughout the work.

Five of these foamed materials (Suspension, Suspension_1, Emulsion, Bulk_0.04, Bulk_0.3 and Dispersion) and a commercial one (V825T) with different molecular weights and polidispersities have been manufactured to later characterize them. With the images obtained by electron microscopy (SEM) and the ImageJ/FIJI analysis-software tool, the relative density has been measured; the average cell size; nucleation density and homogeneity in their structures.

PMMA solid materials have a range of 964.500-63.750 g/mol for molecular weight, 6.4-1.5 for polydispersity and 126.29-114.57 ºC for glass transition temperature.

The manufactured cellular materials present a completely interconnected cellular structure with a wide range in their internal structures. These cover relative densities between 0.15-0.52; cell average sizes between 1.2-73.9 μm and nucleation densities between y $2.9 \cdot 10^7$-$2.9 \cdot 10^{11}$ cells/ cm^3.

The relationship between the obtained cellular structures and the initial characteristics of the synthesized polymers have been stablished.

Keywords: microcellular polymer, poly(methyl-methacrylate); open cell; gas dissolution foaming.

INTRODUCTION:

The study of cellular materials, biphasic materials where a gas is dispersed in a solid phase, commonly known as foams, and specifically cellular polymers [1], has been of great interest in recent decades. These materials exhibit a combination of properties that make them indispensable in many applications.

Cellular polymers offer reduced density, weight, and cost, improved impact energy absorption, buoyancy, and low thermal conductivity, among other properties. These characteristics make them highly sought after in technological sectors such as construction, packaging, automotive, and more. Therefore, controlling the manufacturing process allows to produce tailored materials, which is crucial for the industry [2].

One of the breakthroughs for these materials came in the 1980s at the Massachusetts Institute of Technology (MIT) [3], where the discovery of microcellular polymers through the gas dissolution foaming technique [4] emerged. This method enabled the reduction of cell size in cellular materials from hundreds of micrometres to 10 μm, giving rise to the so-called microcellular materials. Analysing the properties of these new materials [5], which had cell sizes never seen before; a considerable improvement in mechanical properties compared to conventional cellular materials was observed.

Since their discovery, microcellular materials have been manufactured using various polymers, and several of their properties have been studied. Varying the foaming conditions; different structures, densities or cell sizes are achieved. It has been proven that cellular polymers with a finer cell structure have an advantage in mechanical properties against foams with a relatively coarse cell structure [6]. For this reason, microcellular materials have better mechanical properties than standard or macrocellular materials.

In this attempt to reduce cell size and reaching better properties, nanocellular foams have aroused a lot of interest in materials science. These polymeric cellular materials present cell nucleation densities above the 10^{13} nuclei/cm^3 and sizes below 1 μm range. Their small pore size and high specific surface area make them excellent candidates for so many applications. Among them, the most notable one is thermal insulation due to the reduction in gas phase conductivity thanks to the Knudsen effect [7].

Other option for these microcellular and nanocellular materials are the filtering or catalytic applications. However, for this to be possible, it is necessary for a fluid to be able to flow through the interior of the structures, meaning that the cells need to be open and interconnected, which is not common in these materials and is typically achieved by adding a second phase to break the cell walls [8].

The previous properties strongly depend on the characteristics of cellular materials, such as density, cell size, nucleation density, or open cell content. Controlling all these factors depends on the management of the production process.

The most used production route to obtain cellular polymers with these micro and nanocellular characteristics is the gas dissolution foaming process [4] . The gas commonly used is CO_2, due to its green character and good diffusivity and solubility when in its supercritical state, easily achievable (31 °C and 7.3 MPa). The process can be carried out in two different ways: the known "two-step process," a process in two stages, or the one used in this work, the "one-step process," a process in a single stage.

This method consists of four steps: saturation, depressurization, foaming, and stabilization. Firstly, starting from ambient temperature (T_{amb}), the polymer is saturated with CO_2under specific saturation pressure (p_{sat}) and saturation temperature (T_{sat}) conditions (**Fig. 1**). Under these conditions, the gas diffuses into the sample, reaching a state known as saturation. Once the sample is fully saturated within a saturation time (t_{sat}), the gas is rapidly released (v_{desp}) until it reaches atmospheric pressure (p_{atm}) (**Fig. 1**). This creates a significant thermodynamic instability in the gas-polymer system, resulting in phase separation and the appearance of nucleation sites.

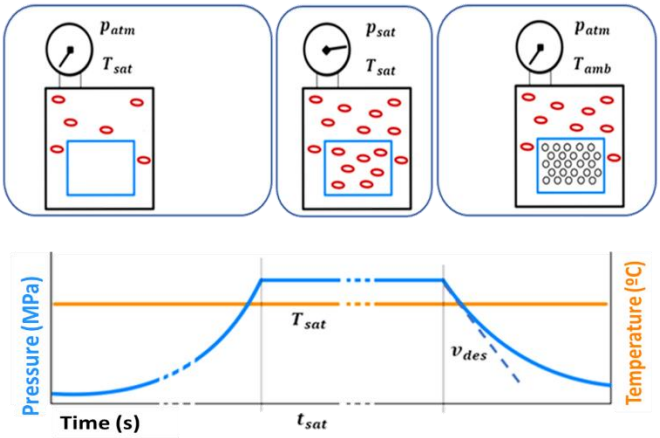

Fig. 1: *One step gas dissolution foaming process.*

To obtain cellular polymers using this technique, mainly two strategies have been followed. One involves using homopolymers (single-phase systems), and the other involves using polymers with a nucleating phase (multiphase systems) following the principles of homogeneous [9] and heterogeneous [10] nucleation mechanisms, respectively.

Despite being the most promising production process, gas dissolution foaming presents some drawbacks. On the one hand, it usually requires long manufacturing times, which poses a disadvantage for industrialization. On the other hand, control the open cell content, when using a solid precursor, is not an easy task, making it difficult to use them in the filters or sensors sectors.

Reducing the viscosity and the glass transition temperature of the sample would be one opportunity to overcome such problems. Gelling the polymer or plasticizing it would lead to this promising characteristic in precursors. Polymeric gels [11] are systems composed of a three-dimensional network of polymers dispersed in a solvent. These polymeric networks consist of long, entangled chains that act as a matrix, retaining the solvent in place and providing solidity to the gel. Polymeric gels can be found in both natural and synthetic forms. Examples of natural gels include the cornea, vitreous humour, and connective tissues in our bodies, which play vital roles in providing structure and support to tissues. In the synthetic realm, a wide variety of polymeric gels with specific properties and applications have been developed. These synthetic gels find applications in fields such as biomedicine, food industry, materials chemistry, and more. Their versatility and ability to retain large amounts of solvent make them promising materials in various scientific and technological fields.

According to literature, foaming different polymers plasticized or diluted in different solvents [12]–[15], which have been manufactured with the technique of solvent – cosolvent and super critical CO_2. In these works, by using 35 – 65ºC and 10 – 25 MPa of saturation temperature and pressure, respectively, 100-300 μm in thickness membranes have been produced presenting cell sizes of $1-25$ μm and with medium-high open cell porosity (74-86%). For crosslinked polymers membranes and acetone [15]of 500 μm using 35 – 75ºC and 25 MPa of saturation temperature and pressure, samples present cell sizes of $1\text{nm}-10$ μm and some not characterized open cell porosity. Saturation times for these membranes are in the range of 20 – 45 min. Such open cell contents are hardly founded for solid polymers, in addition, saturation times for solid polymers 2-4 mm [16] [17] saturated at 24 – 250 ºC and 31 – 32 MPa; are in the range of 20 – 24 hours, presenting cell sizes of $1-25$ μm.

In all the previous membranes works foam structures are directly linked and discussed with the processing conditions and not with polymer characteristics. But to obtain the final desired cellular polymer, additionally to the control of the production process, it is essential to control the characteristics of the polymer matrix such as viscosity, molecular weight. Such polymer properties have been related to the final cellular structure for different commercial polymers in the literature [3], [4], [16]. However, all these works deal with solid precursors for the gas dissolution process and not polymeric gels.

Due to these gaps in the reported literature; this work tries to relate the molecular weight and polydispersity from different-ways tailor-polymerized poly (Methyl-Methacrylate) (PMMA) precursors with final structure of high open-cell porosity (> 85%) thick (millimetric-scale) polymeric foams fabricated through an acetone-PMMA gel in the gas dissolution foaming process.

1. EXPERIMENTAL:

1.1. Materials:

The base material used to manufacture cellular materials is poly (Methyl-Methacrylate) $(C_5O_2H_8)_n$, commonly known as PMMA. This material is a thermoplastic resin obtained through the polymerization of the monomer methyl methacrylate. Since Rohm and Haas Company first produced PMMA in 1933 [18], it has been extensively used in the industrial sector due to its favourable characteristics. It is often used as a substitute for glass because of its high transparency, strength, lightweight nature, and good mechanical properties. PMMA is often used for manufacturing micro and nanocellular samples by gas dissolution foaming due to its excellent behaviour with super critical CO_2. Also, PMMA is well dissolved in acetone. For these reasons is the perfect candidate in this work.

To polymerize PMMA, Methyl methacrylate (MMA), 2,2′-Azobis(2-methylpropionitrile) (AIBN), polyvinyl alcohol (PVOH), Mw 85,000-124,000 and 87-89% hydrolysed, acetone, methanol (MeOH) and potassium persulfate (KPS) were provided by Sigma Aldrich. The reagents were used as received. Chemical reactions and a more detailed discussion and explanation of the processes can be found in the **Appendix 1** after Bibliography.

1.1.1. PMMA polymerization:

The following methods have been used to obtain PMMA with different molecular structure and characteristics:

2.1.1.a. Bulk polymerization:

MMA and AIBN were placed in a 50 mL flask, as indicated in **Tab. 1**. The solution was then deoxygenated using N_2 (g) and heated to 70°C (**Fig. 2a**). It was kept at this temperature for 8 h. The resulting polymer was dissolved in acetone and precipitated by adding MeOH. The mixture was subsequently filtered, and the solid (**Fig. 2b**) was washed with MeOH. Finally, the polymer was dried under reduced pressure for 48 hours at 60°C.

Reference	MMA	AIBN	Ratio AIBN/MMA
BULK_0.3	20 g	6x10-2 g	0.3 %w/w
BULK_0.04	20 g	8x10-3 g	0.04 %w/w

Tab. 1: *Amounts used in obtaining the PMMA samples by the bulk polymerization technique.*

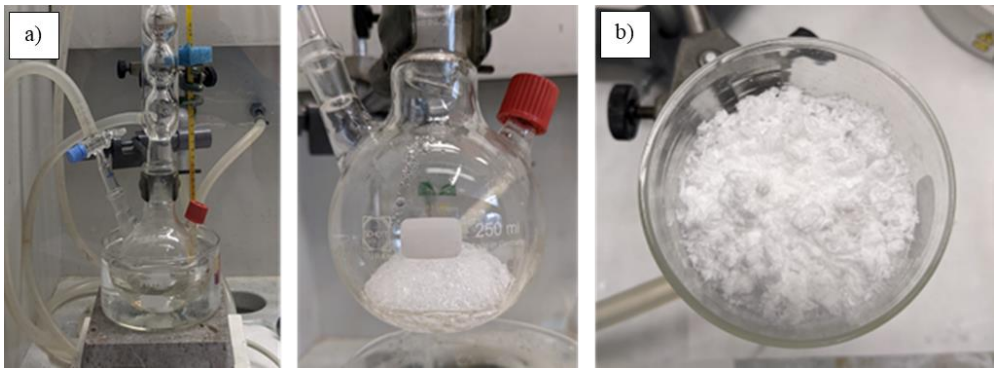

Fig. 2: a) Assembly used during bulk polymerization. b) Polymerized PMMA.

2.1.1.b. Suspension polymerization:

In a two-neck flask (**Fig. 3a**) with a volume of 100 mL, 40 mL of distilled deionized water (DDI H_2O), previously deoxygenated with N_2 (g), and 0.8 g of PVOH (2 g PVOH/dL H_2O) were placed. The flask was maintained under a nitrogen atmosphere as the mixture was heated to the reaction temperature of 64 °C and stirred until a solution was formed. In a separate flask, 12 mL of MMA and 0.0925 g of AIBN (5x10-3 mol AIBN/mol MMA) were combined. The mixture was deoxygenated with N_2 (g) and stirred until a solution was obtained, under nitrogen atmosphere and keeping it cold, ~ 0 °C. The organic solution was then added to the water-PVOH system, and the mixture was kept under an inert atmosphere at 64 °C with constant stirring for 24 hours to allow for polymerization to occur. To promote stabilization of the PMMA particles (**Fig. 3b**), the reaction mixture was cooled and kept at a low temperature. Subsequently, the PMMA particles were separated by centrifugation (**Fig. 3c**) at 10,000 rpm and washed repeatedly with hot water and methanol. The polymer was air-dried and further dried under reduced pressure for 48 hours at 60 °C.

Fig. 3: a) Assembly used during bulk polymerization. b) PMMA particles. c) Thermo Scientific Sorvall X4R Pro MD Refrigerated Centrifuge.

2.1.1.c. Dispersion polymerization:

In a two-neck flask with a volume of 100 mL, 25 mL of deionized water (H_2O /MeOH = 0.5), previously deoxygenated with N_2 (g), and 0.75 g of PVOH were placed. The flask was maintained under a nitrogen atmosphere as the mixture was heated to the reaction temperature of 64 °C and stirred until a solution was formed. Then, 40 mL of methanol (MeOH) and 5 mL of MMA, previously deoxygenated with N_2 (g), were added to the flask. After stirring, 0.05 g of AIBN (6x10-3 mol AIBN/mol MMA), dissolved in 10 mL of MeOH, was incorporated into the mixture. The system was kept under an inert atmosphere at 64 °C with constant stirring for 24 hours to allow for polymerization to occur. Upon completion of the polymerization, the reaction mixture was cooled to promote stabilization of the PMMA particles. Finally, the PMMA particles were separated by centrifugation at 10,000 rpm and washed repeatedly with hot water and methanol. The polymer was air-dried and further dried under reduced pressure for 48 hours at 60 °C.

2.1.1.d. Emulsion polymerization:

In a two-neck flask with a volume of 250 mL, 140 mL of deionized water (DDI H_2O) and 6 mL of MMA (4% v/v with respect to H_2O) were placed. The mixture was deoxygenated using N_2 (g) and heated to the reaction temperature of 60 °C. Then, a solution of 0.045 g of KPS in 10 mL of deionized water (DDI H_2O), previously deoxygenated with N_2 (g), was added to the flask. The system was maintained under an inert atmosphere at 60 °C with continuous stirring for 24 hours to allow polymerization to occur. After completing the polymerization, the reaction mixture was cooled to promote stabilization of the PMMA particles. Subsequently, the PMMA particles were separated by centrifugation at 10,000 rpm and washed repeatedly with hot water and methanol. The polymer was air-dried and further dried under reduced pressure for 48 hours at 60 °C.

2.1.1.e. V825T:

For comparison a commercial PMMA has been used in this work. Bought from ALTUGLAS® International (Colombes, France). V825T (from now on just called VT) characteristics are next to the other PMMA in **Tab. 3**.

2.1.1.f Acetone and sc. CO_2:

Acetone ($CH_3(CO)CH_3$) (purity 99,9%) (bought from Scharlab S. L., Sentmenant, Spain) is an organic polar solvent from the acetone group. In this work it is used as plasticizer for PMMA.

Dioxide carbon (CO_2) (purity 99,9%) (purchased c., Madrid, Spain) is used as blowing agent after pressuring through super critical point.

1.1.2. Gels Preparation:

Before proceeding to manufacture the gels, to improve the solvent capacity of acetone on solid PMMAs, they are pulverized. This increases the surface area exposed to contact with the solvent. A Ball Mill (MM400, Retsch GmbH) (**Fig. 4a**) cooled with liquid nitrogen is used for this purpose during 1 minute at a 29 s^{-1} agitation frequency.

For mixing in a proper way the gels, pulverized PMMA and acetone in a relation of 1:4 in weight is used. For weighting the right amount of both elements to achieve a 3 mm wide gel sample, a precision balance ((Mettler-Toledo) is used (**Fig. 4b**). Then both materials were poured into a cupcake made of filtering paper inside a syringe (as shown in **Fig. 4c**).

Fig. 4: *a) Ball Mill (MM400, Retsch GtolembH). b) Precision balance (Mettler-Toledo). c) Cupcake-syringe system.*

Once materials are in the cupcake inside the syringe, this is closed with another plunger to seal it and prevent acetone evaporation. Agitation of the gel precursor takes place for 24 hours at 2000 rpm in a shaker (Multi Reax, Heidolph Instruments GmbH & Co) like the one shown in **Fig. 5a**. When the gel is homogeneous in appearance, it is pulled out of the syringe. Now a second cupcake (**Fig. 5b**) is placed on top making sure the contact between sample and filtering paper material is perfect and no bubbles are left. This way the gel is embedded between the two filtering papers and ready for the foaming tests.

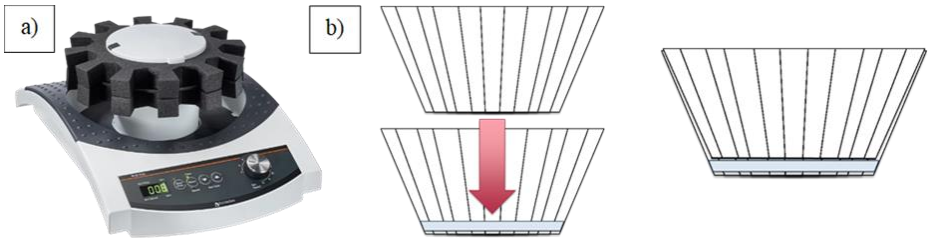

Fig. 5: *a) Shaker (Multi Reax, Heidolph Instruments GmbH & Co). b) Scheme of the PMMA gel embedded between cupcakes.*

1.1. One step gas dissolution foaming process:

To produce cellular materials, the one step gas dissolution foaming method is used. The set-up, schematized in **Fig. 6**, consists mainly of a pressure vessel (PARR 468, Parr Instrument Company, Moline, IL, USA), a pressure pump (SFT-10, Supercritical Fluid Technologies Inc., Newark, DE, USA) that supplies the necessary pressure to the system, and a 1200W thermal jacket connected to a controller (CAL 3000) responsible for temperature control.

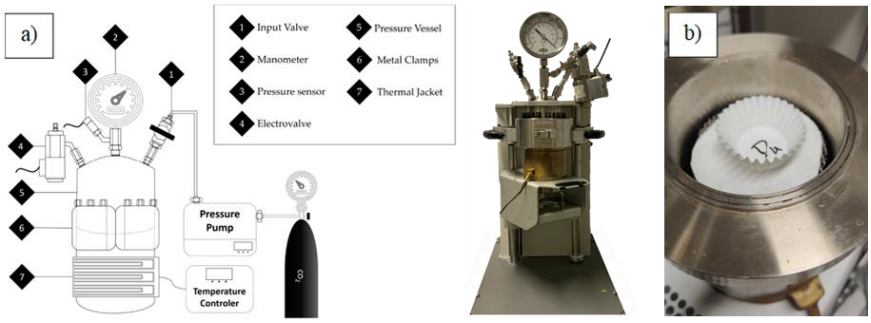

Fig. 6: *a) Set-up scheme and photograph. b) Double cupcake sample inside the pressure vessel.*

During the CO_2 dissolution process the V_{eff} of the pressure vessel has been reduced to 382 cm^3 by including a notch inside. A T_{sat} of 55°C and a p_{sat} of 25 MPa were used to produce all the cellular materials. The sample was held under these conditions for 1 hour. Depressurization was carried out at a depressurization v_{desp} of 100 MPa/s. Due to the reduction of effective glass transition in PMMA by acetone and CO_2, samples expand immediately after the release of pressure.

1.2. Characterization:

1.2.2. PMMA:

2.3.1.a FTIR:

In this work, IR was carried out using Bruker Tenson 27 Infrared spectrophotometer (**Fig. 7**) in the wave region between 4000 to 500 cm^{-1}, resolution 4 cm^{-1}. This technique is used to analyse polymer composition and to show if polymerization processes have been accurate.

Fig. 7: *Bruker Tenson 27 Infrared spectrophotometer.*

2.3.1.b. GPC (Gel Permeation Chromatography):

Number-, weight-average, centrifugation-average molar masses (M_n, M_w, M_z) (**Figure. 8**) and polydispersity index (PDI) ($Đ_a$) from each PMMA are recorded in CHCl3 (Calibrated with PMMA monodisperse standards) Gel Permeation Chromatography. Each of the molecular weights and PDI are calculated according to **Eq. 1- 4**.

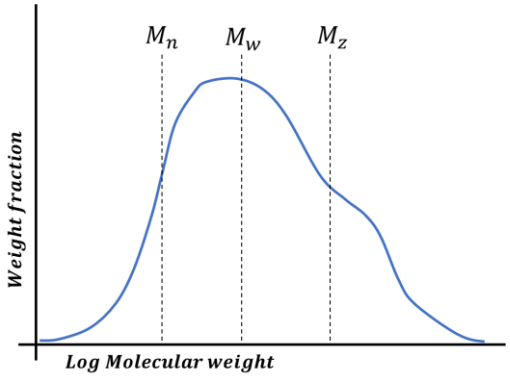

Fig. 8: *Distribution of different molecular weights in a standard GPC graphic.*

$$M_n = \frac{\Sigma N_i M_i}{\Sigma N_i} \quad \textit{(Eq. 1)}$$

$$M_w = \frac{\Sigma N_i M_i^2}{\Sigma N_i M_i} \quad \textit{(Eq. 2)}$$

$$M_z = \frac{\Sigma N_i M_i^3}{\Sigma N_i M_i^2} \quad \textit{(Eq. 3)}$$

$$PDI = \frac{M_w}{M_n} \quad \textit{(Eq. 4)}$$

2.3.1.c. DSC (Differential Scanning Calorimetry):

Glass transition temperature (T_g) from each PMMA were measured by differential scanning calorimetry (DSC) (model DSC822e, Mettler) using a heating programme from 20 ºC to 160 ºC at a rate of 10 ºC/min. The glass transition temperature is then calculated as the mid-point of the drop that characterizes this temperature.

2.3.1.d. TGA (Thermogravimetric Analysis):

Thermogravimetric Analysis is performed in each solid sample of PMMA using a programme from 50ºC to 850ºC at a rhythm of 20ºC/min.

2.3.1.e. Density:

The density of the solid samples was measured using a gas pycnometer (model AccuPyc II 1340, Micromeritics) showed in **Fig. 9a**.

2.3.2. Cellular materials:

After fabrication, samples stayed at room temperature until all the CO_2 and acetone that can remain inside after de foaming process completely diffused out the samples, then characterization was performed.

2.3.2.a. Density:

The density of the corresponding cellular materials was determined with the water-displacement method based on Archimedes' principle. A density determination kit for a Mettler-Toledo balance (**Fig. 9b**) has been used for this purpose. Relative density (ρ_r) (**Eq**.) was calculated as the ratio between the cellular material density (ρ_f) and the density of the corresponding solid polymer (ρ_s).

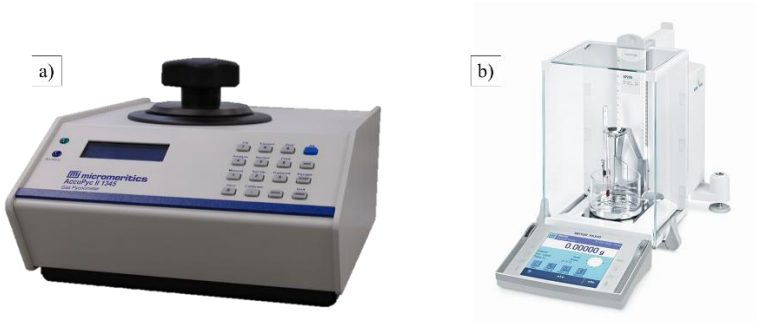

Fig. 9: *a) Pycnometer (AccuPyc II 1340, Micromeritics). B) Mettler-Toledo balance with density kit.*

2.3.2.b Open-cell structure:

Measurement of the interconnected pores proportion as OC % was measured using a gas pycnometer (model AccuPyc II 1340, Micromeritics) and **Eq 5.**

$$OC\% = \frac{V_{ext} - V_{pyc}}{V_{ext}(1-\rho_{rel})} \qquad (Eq.\ 5)$$

Where V_{ext} is the geometrical volume of the cellular material sample, V_{pyc} is the volume measured with the pycnometer and ρ_{rel} is the relative density between the solid and the foam.

2.3.2.c Cellular structure:

To analyse the structure of the cellular samples, a Scanning Electron Microscope (Flex SEM 1000 VP-SEM) as that shown in **Fig. 10a** was used. Before visualization, the materials were cooled in liquid nitrogen to preserve the sample structure and then fractured. Afterward, the samples were coated with gold using a sputter coater (model SCD 005, Balzers Union) (**Fig. 10b**). Structural parameters were quantified using a tool that utilized the ImageJ/FIJI software [19].

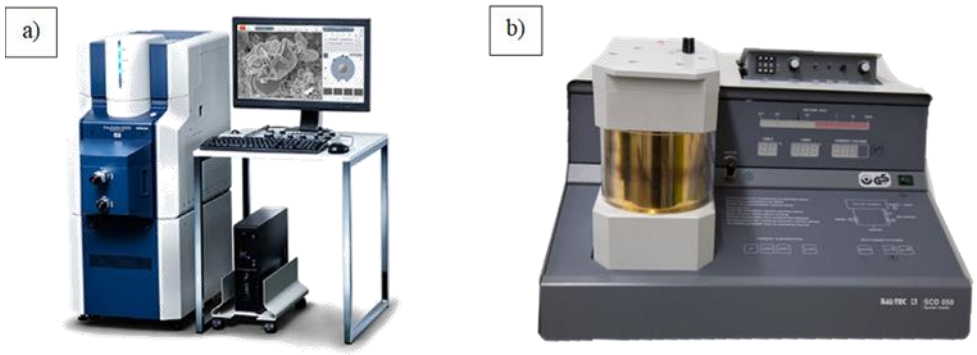

Fig. 10: *a) Scanning Electron Microscope (Flex SEM 1000 VP-SEM). b) Sputter coater (model SCD 005, Balzers Union)*

The following steps were taken to obtain parameters for the structural analysis:

First, the average cell size in 3D (ϕ_{3D}) and standard deviation coefficient of the cell size distribution (SD) was determined. The 3D values were obtained by multiplying the 2D values measured in the image by the correction factor of 1.273 [19]. The normalized standard deviation coefficient (**Eq. 6**) was calculated as an indicator of the homogeneity of the cellular structure, which allows for comparison between materials with different cell sizes. The cell density (N_v) was determined using Kumar's theoretical approximation (**Eq. 7**) [20], where A is the analysed area and n is the number of cells in that area. For each region, over 200 cells were analysed.

$$Homogeneity = \left(\frac{SD}{\phi}\right) \qquad (Eq.\ 6)$$

$$N_v = \left(\frac{n}{A}\right)^{3/2} \qquad (Eq.\ 7)$$

To determine the cell nucleation density (N_0) of the sample, which had homogeneous cells **Eq. 8** was used with the relative density of the core (ρ_r). This relationship assumes that there were no degenerative or coalescence effects on the structure during foaming, meaning that every nucleation point in the solid became a cell in the foamed material.

$$N_0 = \frac{N_v}{\rho_r} \qquad (Eq.\ 8)$$

2. SOLUBILITY THEORY:

The Hansen Solubility theory was developed by Charles Hansen in his Doctoral thesis in 1967 [21]. In this framework, polymers and solvents are represented in a 3D-space by three coordinates called the Hansen Solubility Parameters (HSPs). Each of the parameters is related to the strength of one of the long-distance cohesive forces: polar bonding energy density represented by δ_P, dispersive bonding energy density represented by δ_D, and hydrogen bonding energy density represented by δ_H. Distances in HSP space are calculated using the formula:

$$R_a = \sqrt{4\Delta D^2 + \Delta P^2 + \Delta PH^2} \qquad \textit{(Eq. 9)}$$

Where ΔD, ΔP and ΔH are the differences in the δ_D, δ_P and δ_H parameters between the polymer and the solvent. For polymers as solutes, an additional parameter controls the relation with solvents. The interaction/solubility distance (R_0) is also defined. Solvents within this distance can dissolve the polymer. This term is obtained through experimentation, Molecular Dynamics and algorithms [22]. Thus, for solvents with a distance Ra < R_0 to the polymer, dissolution of the polymer will occur. In the case of PMMA $R_0 = 9.4\ MPa^{1/2}$ for $M_w = 120{,}000\ g/mol$, lower molecular weights will have larger R_0 values, while for larger ones the value of R_0 will be smaller [23].

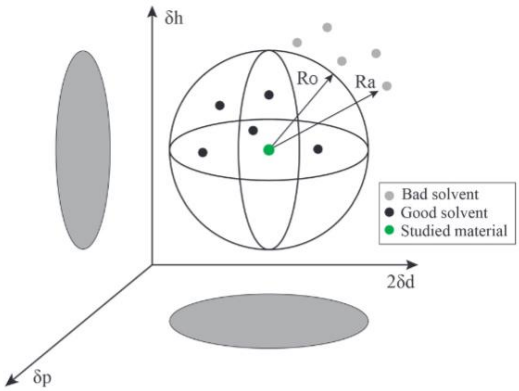

Fig. 11: *Solubility in polymers is calculated using HSP parameters and the Sphere technique* [24].

This approach allows for the prediction of solubility and miscibility behaviour between polymers and solvents based on their HSP values. If the HSP values of a polymer and a solvent are similar or close in HSP space, they are expected to be more likely to dissolve or mix. Conversely, if the HSP values are significantly different, the polymer and solvent may have limited solubility or compatibility.

The Hansen Solubility Parameters provide a useful tool for understanding and predicting the solubility behaviour of polymers in various solvent systems, aiding in the design and formulation of polymer-based materials.

Another concept to mention is the RED value (Relative Energy Difference) given by RED = Ra/Ro. For RED < 1 the solvent is within the ellipsoid, while a RED > 1 means the solvent is outside.

Material	$\delta_P/MPa^{1/2}$	$\delta_P/MPa^{1/2}$	$\delta_H/MPa^{1/2}$	R_a	RED
PMMA	17.9	7.3	7.8	-	-
Acetone	15.5	10.4	7	6.5	0.6
Sc. CO_2	15.6	5.2	5.8	8	0.58

Tab. 2: *Parameters for bonding energies densities at ambient conditions for acetone and at the sc. point for CO_2 (3.37MPa and 304 K).*

This solubility parameters are strongly related to temperature, pressure and the presence of other cosolvents [25] [26], [27]. Some results and mathematical methods have been reported in the literature [28] [29]. Using the molar volume as a reference for temperature and pressure of each solvent (V_{ref}), solubility parameters are calculated (**Eq. 10-12**) for experimental conditions.

$$\frac{\delta_{Dref}}{\delta_D} = \left(\frac{V_{ref}}{V}\right)^{-1.25} \qquad \textit{(Eq. 10)}$$

$$\frac{\delta_{Pref}}{\delta_P} = \left(\frac{V_{ref}}{V}\right)^{-0.5} \qquad \textit{(Eq. 11)}$$

$$\frac{\delta_{Href}}{\delta_H} = \exp\left[-1.32 \cdot 10^{-3}\left(T_{ref} - T\right) - \ln\left(\frac{V_{ref}}{V}\right)^{0.5}\right] \qquad \textit{(Eq. 12)}$$

3. RESULTS AND DISCUSSION:

3.1. SOLID PMMA:

Fig. **12** shows a photograph of the solid samples produced in this work. The materials that have been polymerized for this work are whiter than the VT commercial one because they have pores inside after polymerization (**Fig. 13**). The powder of PMMA is fine processed in the ball mill with the aim of comparison with the polymerized polymers, for a good and quick solution in acetone.

Fig. 12: *Every PMMA precursor used in this work: a) Dispersion. b) Suspension. c) Suspension_1. d) Emulsion. e) Bulk_0.04. f) Bulk_0.3 g) VT pellets. h) processed and powdery material.*

The porosity of the polymerized solids is checked through SEM, as it can be seen in **Fig. 13** all polymers are composed by small particles presenting voids in between.

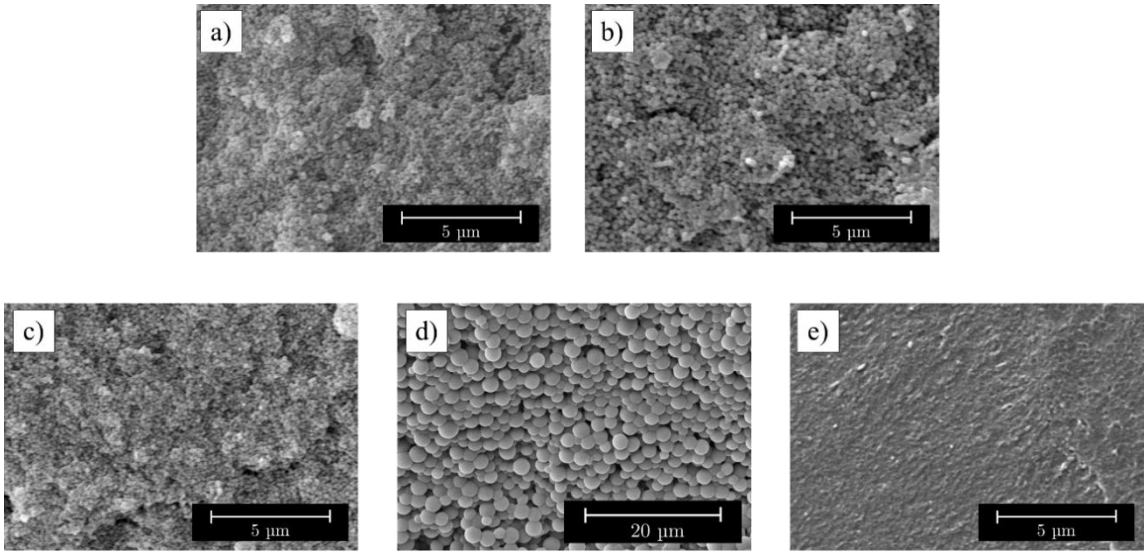

Fig. 12: *Structural differences between solid precursors: a) Suspension_1. b) Emulsion. c) Suspension. d) Dispersion. e) VT.*

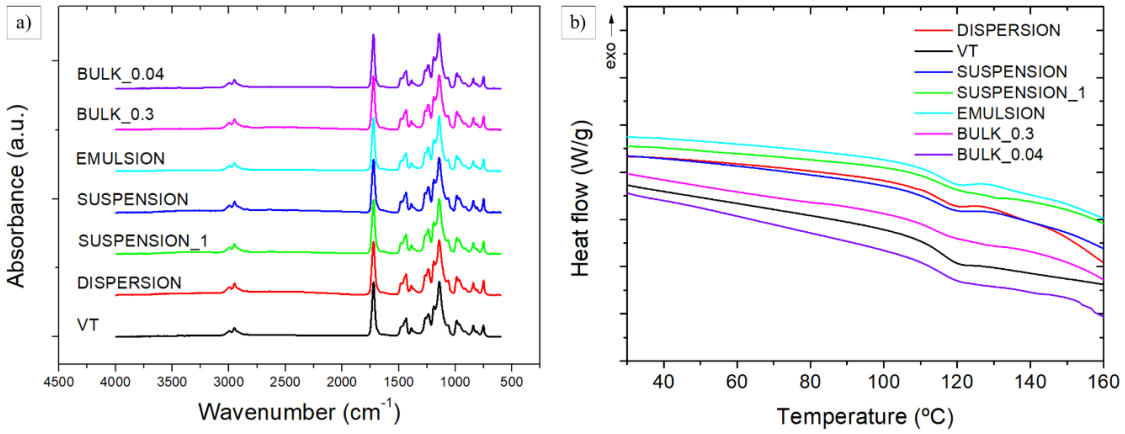

Fig. 13: a) Chemical composition of the samples (FTIR). B) Thermal analysis (DSC).

DSC (**Fig. 14b**) is evaluated in each polymer for determining the glass transition temperature and data is shown in **Tab. 3**. As it can be seen the glass transition temperature is very similar for all the synthesized PMMAs. No conclusions or relation with other parameters could be obtained from that analysis.

Fig. 15a shows the results regarding the TGA analysis of the different polymers. Although **Fig. 15b** shows a narrow peak for the commercial VT PMMA and some impurities in the rest of polymerised materials. These peaks are due to MMA that hasn´t been polymerised, oligomers of MMA or some impurities of chemical agents used in the process. Dispersion polymerization is the one that shows more oligomers due to the use of methanol as solvent, which could have stopped some initial chains to elongate. No residue is left after the heating programme, so there is no charge in the material.

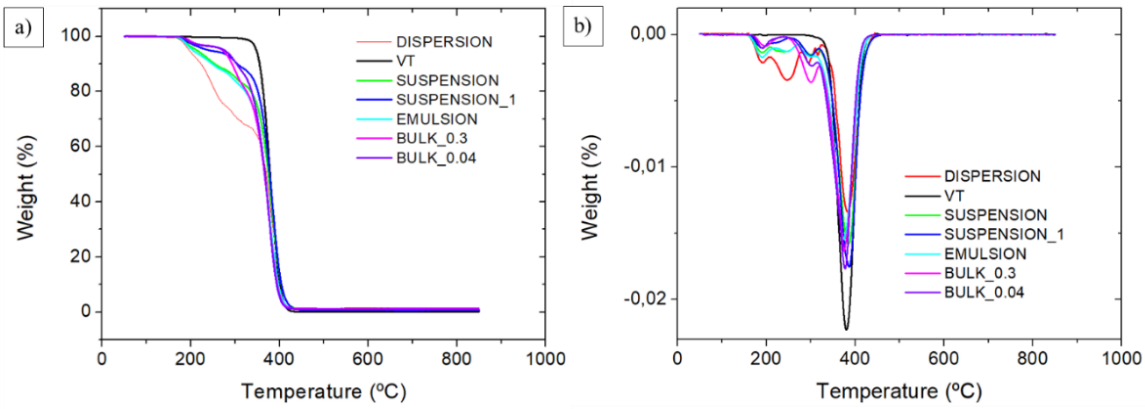

Fig. 14: a) Thermogravimetric data analysis. (TGA). b) First derivative of (TGA).

For determining the molecular weight, their distribution and polydispersity a GPC is realized for each PMMA. **Fig. 15a** shows molecular weight dispersity curves. PMMA materials show such different measures and properties leading to a high diverse group of materials. The interval of molecular weight is 964.500-63.750 g/mol and 6.4-1.5 for polydispersity, this creates such a rich

range of samples. **Fig. 15b** represents M_w and PDI in a single graph. In this way three different regions are separated depending on the polydispersity index (0-2, 2-4, 4-8).

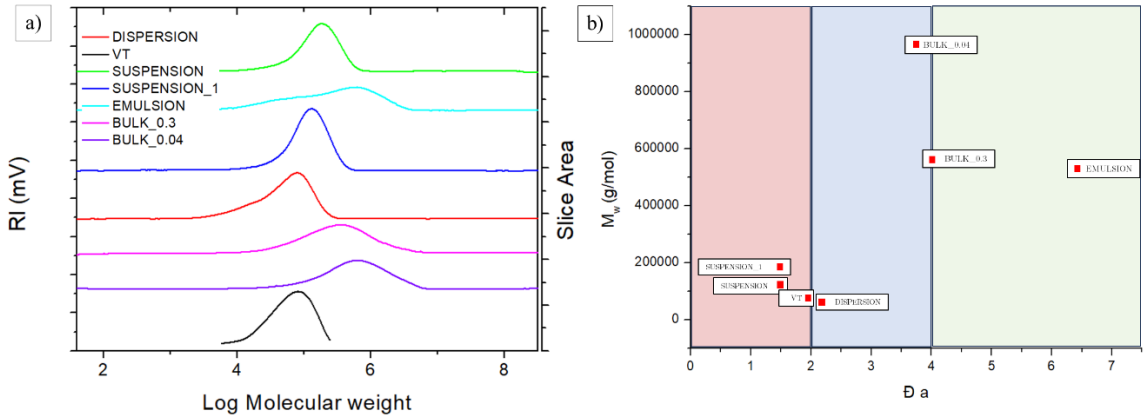

Fig. 15: a) Molecular weight curves distribution due to GPC technique. b) Regions for different $Đ_a$.

Tab. 3 summarizes the number-average molar mass (M_n), mass-average molecular weight (M_w), Z-average molecular weight (M_z) and polydispersity (PDI).

PMMA	T_g (º C)	M_n^a (g/mol)	M_w^a (g/mol)	M_z^a (g/mol)	PDI
BULK_0.3	123.82	141,800	566,200	1,191,600	4.0
BULK_0.04	124.58	260,232	964,500	2,432,450	3.7
Suspension_1	126.29	115,290	177,450	241,100	1.5
Emulsion	120.35	81,800	530,750	1,462,950	6.4
Suspension	123.20	83,800	126,450	169,200	1.5
Dispersion	120.42	29,550	63,750	95,600	2.2
VT	114.57	43,157	83,221	119,283	1.9

Tab. 3: Glass transition temperature, molar masses from each PMMA and polydispersity.

Rheology is affected not only by the molecular weight but the PDI and the polymer branching. A higher molecular weight would lead to higher static viscosity.

These can be explained by two main reasons: Chemically, longer chains achieve more Van der Waals forces and cohesive energy due to more points of interaction between chains. Physically, longer chains arise topological entanglements between them creating a "physical crosslinking" (**Fig. 16**). This effect hinders the "reptation" movement [30] of polymeric chains.

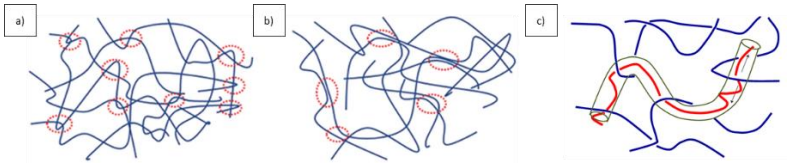

Fig. 16: a) Topological entanglement. B) Cohesion entanglement due to Van der Waals forces. C) One dimension possibility of movement of reptation.

On the contrary, a lower PDI would increase the static viscosity of the polymer. Thus, the higher the molecular weight and the lower the PDI the higher the viscosity. On the other hand, the strain hardening of the polymer improves with a broad molecular weight distribution [31], [32]. A polymer with strain hardening increases its viscosity in extensional flow as elongation increases, being a good candidate for foaming, because it will support expansion. Thus, the higher the PDI the higher the strain hardening. Branching is also very important in rheology, but this data is not available in this study.

Different molecular weight and molecular weight distributions have been obtained thanks to the different polymerization methods. The quantity of initiator, the duration of polymerization, the temperature, the agitation velocity, the solvent media, and the chosen process of polymerization affects to the molecular weight and polydispersity of the final polymer. Firstly, more proportion of initiator leads to lower molecular weights due to a higher density in starting points and shorter chains at the end of the process. This is exposed in M_n in Bulk_0.3 (141.800 g/mol) which has less initiator than Bulk_0.04 (260.232 g/mol) samples [33], [34]. These methods where there is not an aqueous phase usually are characterized by a worst homogeneity mixing process because of an increment in viscosity. This tend to be reflected in higher PDI (4.0 and 3.7) than the other used methods.

Suspension_1 (115.290 g/mol) process was not as clear as Suspension (83.000 g/mol) because the agitation magnet was not big enough to mix the solution [35], [36]. This reflects on a higher molecular weight due to a poor interaction between initiator and monomer generating new chains. On the other hand, the use of MeOH in dispersion (63.750 g/mol) generates polymers with less M_n in comparison with suspension (83.800-115.290 g/mol) where is not used. This is explained due to interactions between the solvent and the initiator helping to a better dispersion and decomposition, once again leading to the creation of new chains [37]. The process of dispersion polymerization is divided into a particle nucleation stage and a particle growth stage. However, unlike other heterogeneous polymerizations, the particle nucleation stage occurs in a homogeneous phase. Due to the concentration rate of MeOH, polymerization take place by emulsion, but also by dispersion leading to a bimodal molecular weight distribution and high PDI (6.4) [38].

3.2. Gel PMMA materials:

Using **Eq. 10-12** HSP are calculated and exposed in **Tab. 4**.

Material (328.15K/25MPa)	$\delta_P/Pa^{1/2}$	$\delta_P/MPa^{1/2}$	$\delta_H/MPa^{1/2}$	R_a	RED
Acetone	14.7	10.2	6.5	7.1	0.75
Sc. CO_2	10.4	4.4	5.4	15.5	1.65

Tab. 4: *Parameters for bonding energies densities at experimental conditions of 55ºC and 25MPa.*

Polymeric chains are considered as big molecules so no modification in its parameters is calculated. Acetone continues being a good solvent for PMMA ($M_w = 120{,}000\ g/mol$) (RED < 1) at experimental conditions (exp), but sc. CO_2 reduces its solvent capacity for PMMA due to the increment of pressure and temperature from super critical point (**Fig. 17**). It is important to say that the effect of a cosolvent as acetone with sc. CO_2 results in a better solubility [39]. This effect is happening in the gels because most of the solvent in this work case is the Acetone and not the sc. CO_2, used just as blowing agent. Achieving a proximate solubility parameter as the Acetone ones

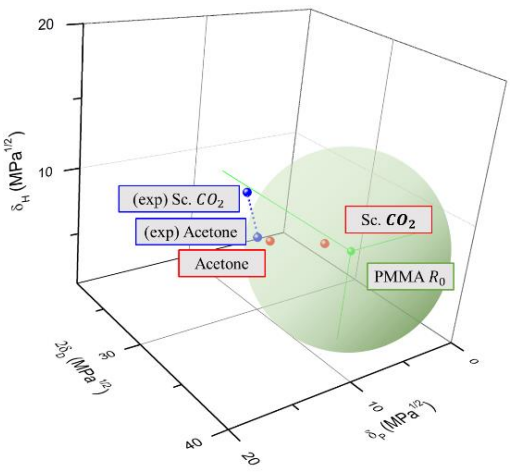

Fig. 17: HSP representation for PMMA and materials in this work at raw conditions and at experimental conditions. Also, mixture of acetone and sc. CO_2 is represented.

Tab. 5 exposes RED relation between PMMA and different wt% ratio of acetone and sc. CO_2. Data shows solubility continues being good for PMMA over 70 wt% of acetone. This is just what happens in gels inside the pressure vessel, a gel 1:4 of PMMA and acetone is saturated with much less wt% content of sc. CO_2 than acetone. Using gelled PMMA by acetone in Gas dissolution foaming increases sc. CO_2 solubility physically, by plasticizing PMMA and reducing viscosity; and chemically as HSP shows. This reduces t_{sat} drastically in just one hour.

wt % Acetone	δ_D/MPa$^{1/2}$	δ_P/MPa$^{1/2}$	δ_H /MPa$^{1/2}$	R_a	RED
100	14.74	10.19	6.51	7.09	0.75
90	14.31	9.62	6.4	7.71	0.82
80	13.87	9.04	6.29	8.42	0.89
70	13.43	8.46	6.18	9.19	0.98
60	13	7.88	6.06	10.01	1.06
50	12.56	7.31	5.95	10.88	1.15
40	12.13	6.73	5.84	11.77	1.25
30	11.69	6.15	5.73	12.69	1.35
20	11.25	5.57	5.62	13.63	1.45
10	10.82	5	5.51	14.58	1.55
0	10.38	4.42	5.39	15.55	1.65

Tab. 5: Solubility parameters and ability to solve PMMA depending on the percentage of sc. CO_2 and acetone.

There will be times when the HSP will say that a given solvent blend will dissolve a certain polymer, but experiments show that it merely swells. This is because its excessively high

molecular weight means that it will take far too long to dissolve it and so only swells it. This is because R_0 of the polymer has been determined using a low molecular weight, then it is entropically probable that solvents which were just good enough for the low molecular weight version will be inadequate for the high molecular weight. The need for a solvent closer to the HSP of the polymer, or for a solvent with a lower molar volume, is therefore predictable. So, this election of $R_0 = 9.4\ MPa^{1/2}$ for PMMA is data for $M_w = 120{,}000\ g/mol$.

A gel is fabricated from each PMMA. The viscosity of each gel is very different as it is shown in **Fig. 18**. Commercial grade VT, present a low viscosity in comparison to Bulk_0.04 and Suspension, that present medium and high viscosities. VT has the lower molecular weight together with a low PDI, leading to this low viscosity of the gel. However, Bulk_0.04 with a much higher molecular weight is less viscous than Suspension, which can be explained due to the higher PDI of Bulk_0.04 material.

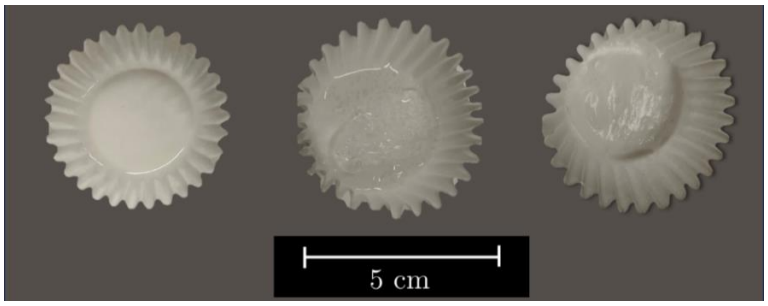

***Fig. 18*:** *Three different consistencies in gel viscosity: low (VT), medium (Bulk_0.04) and high (Suspension).*

M_w and PDI are fundamental variables for viscosity in polymer, as previously explained, and therefore for dissolving. Higher molecular weights lead to longer polymeric chains and more viscosity, as well as low PDI, leading therefore to also more viscous gels. Monodisperse samples (< PDI) lead to less free volume [40] between chains, reducing the space for solvent molecules to locate and dissolve the PMMA. Dissolution process is a nonlinear process in space and in molecular weight [41]. Different layers (infiltration layer, solid swollen layer, gel layer and liquid layer) between the solvent and the PMMA are created while the solvent diffuses and creates holes and channels. Then the polymer chains, which are more mobile due to the presence of solvent, disentangle from the surface of the swollen polymer and diffuse into the bulk solvent [42].

Also, larger molecular weights chains yield higher levels of disentanglement. Therefore, these molecular weights have a higher degree of swelling before dissolution occurs. Shorter chains dissolve at a faster rate than longer chains and, after their removal, solvent penetrates deeper in the polymer. Then longer chains can be affected by solvent which has penetrated faster thanks to those shorter chains. So PMMAs with lower M_w and higher PDI is dissolved quicker in acetone. VT is dissolved in less than an hour at 1500 rpm agitation, both Bulk in 8h and both Suspension in more than 24h.

3.3. Cellular PMMA materials:

Cellular materials produced through gas dissolution foaming have different thickness (although the initial gel thickness was the same) (**Tab. 6**) due to the different expansion rate or the initial PMMA quantity in gels. In the case of VT material, viscosity was extremely low so most of the gel was lost through the bottom cupcake paper during the hour inside the pressure vessel.

A general image of the thickness of the obtained materials are shown in **Fig. 19**, all the materials have a homogeneous structure across the entire sample, except for the Suspension_1 which is not well saturated due to low PDI and so high viscosity resulting in smaller diffusivity of the gas, so the used saturation time is not enough for this sample (**Fig. 19**).

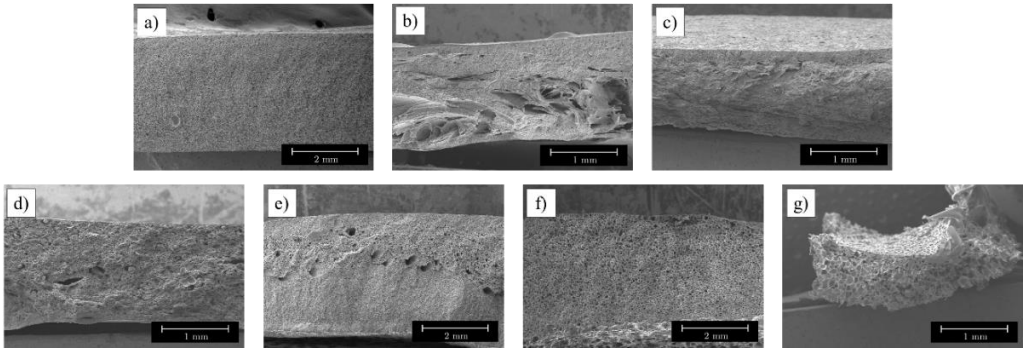

Fig. 19: *Macroscopic SEM images of different cellular PMMA: a) BulK_0.03. b) Bulk_0.04. c) Suspension_1. d) Suspension. e) Emulsion. f) Dispersion. g) VT.*

The obtained relative density can be seen in **Tab. 6** and they go from 0.15±0.01 to 0.52±0.01.

PMMA	ρ_{foam} (g/cm^3)	ρ_{rel} (g/cm^3)	Thickness (µm)
BULK_0.3	0.33±0.01	0.24±0.01	2.29±0.16
BULK_0.04	0.6±0.01	0.49±0.01	1.36±0.05
Suspension_1	0.7±0.01	0.52±0.01	1.12±0.08
Emulsion	0.32±0.01	0.22±0.01	2.51±0.11
Suspension	0.58±0.01	0.40±0.01	1.34±0.04
Dispersion	0.26±0.01	0.18±0.01	2.46±0.04
VT	0.18±0.01	0.15±0.01	0.69±0.08

Tab. 6: *Densities and thickness of the* cellular material *samples.*

In the case of Suspension_1 its high density (0.52±0.01 g/mol) is due to the not saturated and not foamed nuclei of the sample. For the rest of the samples, density values are directly related with the obtained cellular structure, cell size and cell nucleation density, which are indicated in **Tab.7.** and showed in **Fig.21.** As it can be seen, commercial PMMA, VT (0.15±0.01 g/mol) has the highest expansion rate and clearest the biggest cell sizes. For the rest of the polymerized PMMAs materials with the lowest densities are such with the highest cell sizes and lowest cell nucleation densities.

PMMA	ρ_{rel} (g /cm^3)	ϕ_{cell} (μm)	Homogeneity	N_0 (cells/cm^3)	OC %
BULK_0.3	0.24±0.01	9.6±4.3	0.45	$5.2 \cdot 10^9$	98%
BULK_0.04	0.49±0.01	1.9±1.2	0.63	$2.9 \cdot 10^{11}$	82%
Suspension_1	0.52±0.01	1.2±1.1	0.87	$9.9 \cdot 10^{10}$	-
Emulsion	0.22±0.01	8.9±4.3	0.48	$5.4 \cdot 10^9$	98%
Suspension	0.40±0.01	3.8±3.3	0.86	$2.2 \cdot 10^{10}$	92%
Dispersion	0.18±0.01	48.8±12.5	0.25	$5.1 \cdot 10^7$	100%
VT	0.15±0.01	73.9±30.1	0.41	$2.9 \cdot 10^7$	86%

Tab. 7: *Cell sizes, homogeneity index and nucleation density of the cellular material samples.*

As shown in **Tab. 7** all the materials foamed by gas dissolution process are in the microcellular range, with cell sizes between 1.21±1.06 and 73.98±30.06 μm and cell nucleation densities from $2.9 \cdot 10^7$ to $2.9 \cdot 10^{11}$ nuclei/cm^3. The large open cell content of all the materials stands out, as it can be seen values above 86 % are obtained for all the materials. Such values are very unlike for PMMA microcellular foams obtained through gas dissolution foaming with the solid (no acetone) polymer. Additionally, it is worthy to notice the small pores connecting cells. Although cells are in the microcellular range, the interconnecting holes present sizes in the nanometric range, this characteristic is such interesting for some properties of the material. An in deep study of the interconnecting holes is described in **Appendix 2** after Bibliography).

Regarding homogeneity, all the materials have a homogeneous structure across the entire sample, except for the Suspension_1 (not saturated). In the case of Suspension sample, lower M_w than Suspension_1, and so less viscosity; allows cell structure to be generated under these conditions. These cells have the lowest homogeneity (**Eq. 6**) 0.87, illustrating that for so low PDI; lower M_w is necessary for achieving a good quality structure (**Fig. 20**). Also, Bulk_0.04 has some structural defects due to the so high M_w, this is also reflected in low homogeneous structure (0.63). But in comparison, Dispersion is the most homogeneous material fabricated (0.25). Emulsion has some small defects because of the presence of oligomers and some impurities from polymerization processes in presence of solvents and aqueous medias (0.48).

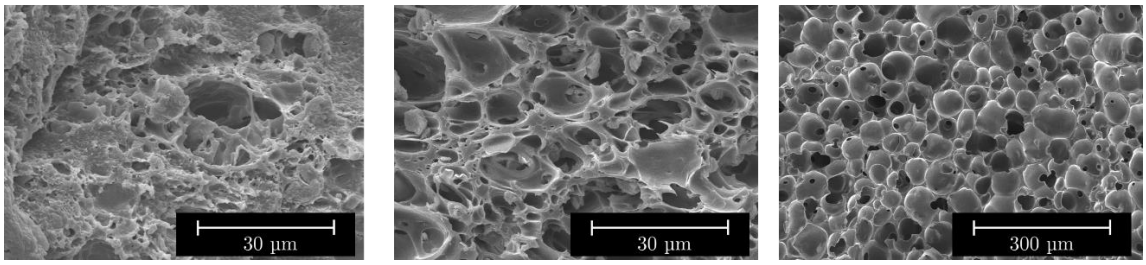

Fig. 20: *Detailed SEM images:* a) *High content of solid phase in* Suspension_1. B) Slow homogeneity in Suspension. c) High homogeneity in Dispersion.

In order to relate the obtained cellular structure with the properties of the polymerized PMMA, the obtained cellular structures are represented with the M_w and PDI of each polymer in **Fig.21.**

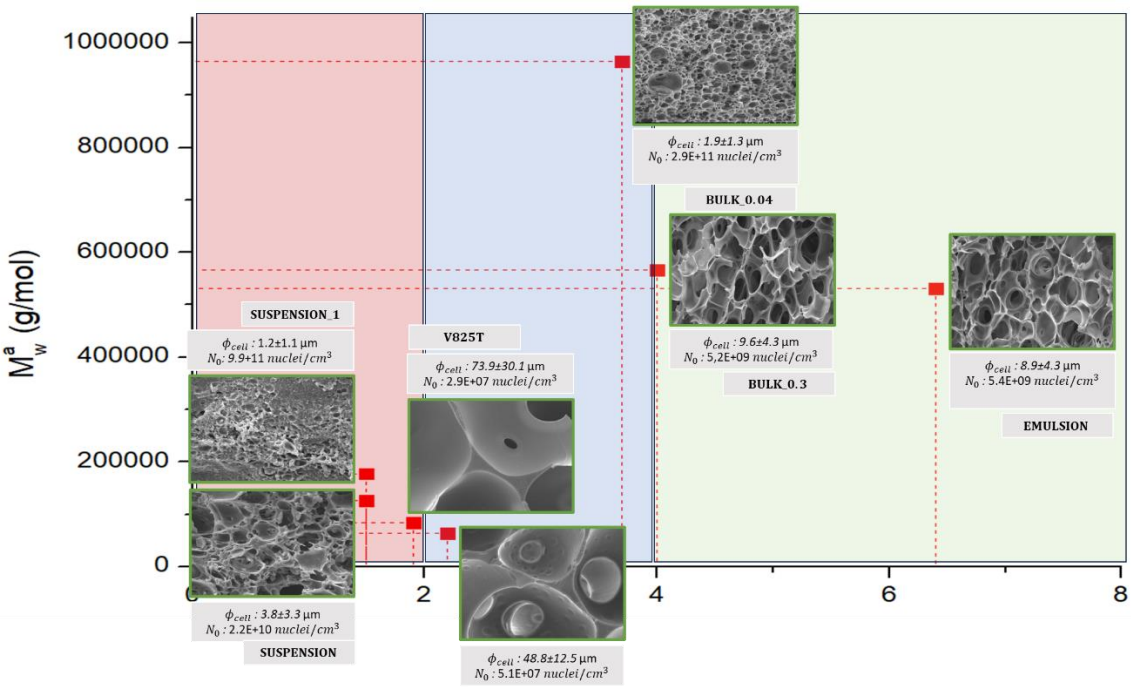

Fig. 21: *Cellular materials structures next to M_w and $Đ_a$ of each polymer.*

Data show two grades of dependence for cellular structure (ϕ_{cell} and N_0), molecular weight (M_w) and polydispersity index (PDI). Understanding them separately is important for generating the structure wanted for a desire case.

Suspension and Suspension_1 structures are already explained presenting a non-saturated structure and a low homogeneity respectively, being such materials difficult to compare with. For comparing the rest of the cell structures three groups are created: LM – low M_w (< 400.000 g/mol) (VT and Dispersion), MM-medium M_w (400.000-800.000 g/mol) (Bulk_0.3 and Emulsion) and HM – high M_w (> 800.000 g/mol) (Bulk_0.04).

As shown in literature, higher M_w in polymer samples lead to smaller cell sizes (ϕ_{cell}) and higher nucleation densities (N_0) [43]. That is why these three groups reveal to be so important in ϕ_{cell} ranges, tens of inches for LM (VT: 73.9±30.1 µm and Dispersion: 48.8±12.5 µm), couple of inches (Bulk_0.3: 9.6±4.3 and Emulsion: 8.9±4.3 µm) for MM and just Bulk_0.04: 1.9±1.2 µm for HM.

On the other hand, this work proves that PDI have an important role in cellular structure of polymeric materials. From "reptation theory" [30] the smaller polymeric chains contribute to "lubricate" the rest of long chains, generating more flexibility, reptation and less viscosity gels, this allows generating a cellular structure for materials with molecular weights as high as the

Bulk_004 (it is the very first time in literature that PMMA with such a M_w is foamed in a controlled way and giving as a result a homogeneous structure.). In addition, as before explained, a higher PDI improves the rheological behaviour of the polymer, increasing the strain hardening and therefore, decreasing the degeneration and coalescence mechanisms, for this reason for LM; the higher PDI in Dispersion (2.2) creates structures with smaller cell size and higher cell density (ϕ_{cell}: 73.9±30.1 µm and N_0: 5.01E+07 nuclei/cm^3) than the VT (1.95) (73.9±30.1 µm and N_0: 2.9E+07 nuclei/cm^3) ones. Same happens for MM in the case of much higher PDI in Emulsion (6.4) structure (ϕ_{cell}: 8.9±4.3 µm and N_0: .84E+09 nuclei/cm^3) than Bulk_0.3 with 4.0 PDI (9.6±4.3 µm and 8.1E+10 nuclei/cm^3) ones.

4. CONCLUSIONS:

Microcellular materials using PMMA/acetone gels have been fabricated by gas dissolution foaming. It has been shown that controlling molecular weight and PDI leads to gels with different characteristics and finally cellular material samples with high open cell structure and "à la carte" cellular structures with constant foaming experimental conditions.

PMMAs synthesized in this work are in the range of 964.500-63.750 g/mol for molecular weight, 6.4-1.5 for polydispersity and 126.29-114.57 ºC for glass transition temperature. It has been demonstrated that the higher quantity of initiator leads to lower molecular weight. Bulk polymerization results in higher polydispersity, because of a more viscous process by the absence of an aqueous phase. Dispersion generates polymers with less M_w, due to the capability of MeOH in solving and dispersing MMA. Emulsion process results in the highest PDI since bimodal polymer is fabricated, polymerization take place by emulsion, but also by dispersion. Suspension polymerization is the cleanest and narrowest molecular weight distribution because of using PVOH as anti-caking agent. Materials with a high molecular weight and low PDI would have a higher viscosity, while high PDI would improve the strain hardening of the polymer.

Solubility in polymers is influenced by the chemical relation between solvent and solute. It has been demonstrated by HSP, that acetone is a good solvent for PMMA in experimental conditions (RED_{exp}: 0.75); first sweeling polymeric chains and then dissolving them. Also M_w and PDI are crucial parameters in solubility processes. Lower M_w chains are solved easier and quicker than higher ones. Monodispersed polymers, with low reptation capability and small free volume between equal size chains; lead to high viscosity gels and longer dissolving times. For high M_w PMMAs, short chains characteristic from high PDI; acting as lubricant between longer ones. Also sc. CO_2 is a good solvent and blowing agent for PMMA, combining it with acetone; improves its proficiency (RED_{exp} < 1.65). Acetone plasticises the PMMA reducing it T_{geff} and viscosity, then polymeric chains have more mobility and more free volume available for CO_2 is lead.

Cellular materials are produced from the gels. Cell sizes are in a range between 1.21±1.06 and 73.98±30.06 µm and cell density run from 2.86E+07 to 2.92E+11 nuclei/cm^3. Relative densities go from 0.22 to .0.52. Molecular weight and polydispersity take an important role in nucleation processes. On the one hand, lower M_w materials result in bigger ϕ_{cell} and smaller N_0. On the other hand, higher M_w materials result in smaller ϕ_{cell} and larger N_0. In addition, PDI also affects cellular structures, monodisperse polymers generate solid phase in materials and inhomogeneous cells. Polymers with the same M_w and higher PDI leads to smaller cell sizes and higher cell nucleation densities due to the improved rheological properties. All the produced materials present a completely interconnected cellular structure due to the use of acetone.

In conclusion, completely open cellular structures can be obtained through gas dissolution foaming of PMMA/acetone gels. The final cellular structure can be tailored by means of the molecular weight and the molecular weight distribution.

For future work, the rheology of the synthesized polymers and produced gels would be measured to corroborate the given hypothesis. In addition, different acetone contents and production conditions will be tested.

5. BIBLIOGRAPHY:

[1] L. J. Gibson and M. F. Ashby, "Cellular Solids: Structure & Properties," *Advances in Polymer Technology*, vol. 9, no. 2, 1989.

[2] H. Kargarzadeh *et al.*, "Recent developments in nanocellulose-based biodegradable polymers, thermoplastic polymers, and porous nanocomposites," *Progress in Polymer Science*, vol. 87. 2018. doi: 10.1016/j.progpolymsci.2018.07.008.

[3] J. E. Martini-Vvedensky, N. P. Suh, F. Church, and F. A. Waldman, "54) MICROCELLULAR CLOSED CELL FOAMS AND THER METHOD OF MANUFACTURE," 1984.

[4] Martín-De León J and M. Ángel Rodríguez-Pérez, "TESIS DOCTORAL: UNDERSTANDING THE PRODUCTION PROCESS OF NANOCELLULAR POLYMERS BASED ON PMMA DRIVEN BY A HOMOGENEOUS NUCLEATION."

[5] D. I. Collias, D. G. Baird, and R. J. M. Borggreve, "Impact toughening of polycarbonate by microcellular foaming," 1994.

[6] J. Fu, C. Jo, and H. E. Naguib, "Effect of Processing Parameters on Cellular Structures and Mechanical Properties of PMMA Microcellular Foams," 2005.

[7] B. Notario, J. Pinto, E. Solorzano, J. A. De Saja, M. Dumon, and M. A. Rodríguez-Pérez, "Experimental validation of the Knudsen effect in nanocellular polymeric foams," *Polymer (Guildf)*, vol. 56, 2015, doi: 10.1016/j.polymer.2014.10.006.

[8] Victoria Bernardo, Judith Martin-de Leon, and M. Ángel Rodríguez-Pérez, "Highly anisotropic nanocellular polymers based on tri-phasic blends of PMMA with two nucleating agents".

[9] J. S. Colton and N. P. Suh, "The nucleation of microcellular thermoplastic foam with additives: Part II: Experimental results and discussion," *Polym Eng Sci*, vol. 27, no. 7, 1987, doi: 10.1002/pen.760270703.

[10] P. Spitael, C. W. Macosko, and R. B. McClurg, "Block copolymer micelles for nucleation of microcellular thermoplastic foams," *Macromolecules*, vol. 37, no. 18, 2004, doi: 10.1021/ma049712q.

[11] O. E. Philippova and A. R. Khokhlov, "1.13 - Polymer Gels," in *Polymer Science: a Comprehensive Reference: Volume 1-10*, Elsevier, 2012, pp. 339–366. doi: 10.1016/B978-0-444-53349-4.00014-5.

[12] E. Reverchon, E. S. Rappo, and S. Cardea, "Flexible supercritical CO2-assisted process for poly(methyl methacrylate) structure formation," *Polym Eng Sci*, vol. 46, no. 2, pp. 188–197, Feb. 2006, doi: 10.1002/pen.20438.

[13] D. dong Hu, Y. Gu, T. Liu, and L. Zhao, "Microcellular foaming of polysulfones in supercritical CO2 and the effect of co-blowing agent," *Journal of Supercritical Fluids*, vol. 140, pp. 21–31, Oct. 2018, doi: 10.1016/j.supflu.2018.05.017.

[14] E. Reverchon and S. Cardea, "PVDF-HFP membrane formation by supercritical CO2 processing: Elucidation of formation mechanisms," *Ind Eng Chem Res*, vol. 45, no. 26, pp. 8939–8945, Dec. 2006, doi: 10.1021/ie051396w.

[15] R. Oberhoffer and A. Müller, “PRODUCTION OF POROUS MATERIALS BY THE EXPANSION OF POLYMER GELS,” 2014.

[16] J. Martín-De León, V. Bernardo, E. Laguna-Gutiérrez, and M. Ángel Rodríguez-Pérez, “Influence of the viscosity of poly(methyl methacrylate) on the cellular structure of nanocellular materials,” 2019, doi: 10.1002/pi.5920.

[17] J. Pinto, M. Dumon, M. A. Rodriguez-Perez, R. Garcia, and C. Dietz, “Block copolymers self-assembly allows obtaining tunable micro or nanoporous membranes or depth filters based on PMMA; Fabrication method and nanostructures,” *Journal of Physical Chemistry C*, vol. 118, no. 9, pp. 4656–4663, Mar. 2014, doi: 10.1021/jp409803u.

[18] H. J. Staehle and C. Sekundo, “The Origins of Acrylates and Adhesive Technologies in Dentistry.,” *J Adhes Dent*, vol. 23, no. 5, 2021, doi: 10.3290/j.jad.b2000209.

[19] J. Pinto, E. Solórzano, M. A. Rodriguez-Perez, and J. A. De Saja, “Characterization of the cellular structure based on user-interactive image analysis procedures,” *Journal of Cellular Plastics*, vol. 49, no. 6, pp. 555–575, 2013, doi: 10.1177/0021955X13503847.

[20] V. Kumar and N. P. Suh, “A process for making microcellular thermoplastic parts,” *Polym Eng Sci*, vol. 30, no. 20, 1990, doi: 10.1002/pen.760302010.

[21] Charles M. Hansen, “THREE DIMENSIONAL SOLUBILITY PARA METER AND SOLVENT DIFFUISION.”

[22] G. C. Vebber, P. Pranke, and C. N. Pereira, “Calculating hansen solubility parameters of polymers with genetic algorithms,” *J Appl Polym Sci*, vol. 131, no. 1, Jan. 2014, doi: 10.1002/app.39696.

[23] A. M. Gaikwad, Y. Khan, A. E. Ostfeld, S. Pandya, S. Abraham, and A. C. Arias, “Identifying orthogonal solvents for solution processed organic transistors,” *Org Electron*, vol. 30, pp. 18–29, Mar. 2016, doi: 10.1016/j.orgel.2015.12.008.

[24] E. P. Ollé, J. Casals-Terré, J. A. L. Martínez, and J. Farré-Lladós, “Hansen Solubility Parameters (HSPs): A Reliable Tool for Assessing the Selectivity of Pristine and Hybrid Polymer Nanocomposites in the Presence of Volatile Organic Compounds (VOCs) Mixtures,” *Macromol Mater Eng*, Mar. 2022, doi: 10.1002/mame.202200511.

[25] L. L. Williams, “0 Determination of Hansen Solubility Parameter Values for Carbon Dioxide,” 2007.

[26] L. Segade, “Equilibrio líquido-vapor de la mezcla CO2/acetona entre 10ºC y 80ºC,” *La investigación del Grupo Especializado de Termodinámica de las Reales Sociedades Españolas de Física y Química.*, pp. 145–155, 2018.

[27] D. F. Tirado and L. Calvo, “The Hansen theory to choose the best cosolvent for supercritical CO2 extraction of B-carotene from Dunaliella salina,” *Journal of Supercritical Fluids*, vol. 145, 2019, doi: 10.1016/j.supflu.2018.12.013.

[28] M. Zhang, M. Dou, M. Wang, and Y. Yu, “Study on the solubility parameter of supercritical carbon dioxide system by molecular dynamics simulation,” *J Mol Liq*, vol. 248, 2017, doi: 10.1016/j.molliq.2017.10.056.

[29] M. Zhang, M. Dou, M. Wang, and Y. Yu, “Study on the solubility parameter of supercritical carbon dioxide system by molecular dynamics simulation,” *J Mol Liq*, vol. 248, 2017, doi: 10.1016/j.molliq.2017.10.056.

[30] E. Van Ruymbeke, R. Keunings, V. Stéphenne, A. Hagenaars, and C. Bailly, “Evaluation of reptation models for predicting the linear viscoelastic properties of entangled linear polymers,” *Macromolecules*, vol. 35, no. 7, pp. 2689–2699, Mar. 2002, doi: 10.1021/ma011271c.

[31] Ester Laguna Gutiérrez and M. A. Rodríguez-Pérez, “UNDERSTANDING THE FOAMABILITY OF COMPLEX POLYMERIC SYSTEMS BY USING EXTENSIONAL RHEOLOGY.”

[32] G. J. Nam, J. H. Yoo, and J. W. Lee, “Effect of long-chain branches of polypropylene on rheological properties and foam-extrusion performances,” *J Appl Polym Sci*, vol. 96, no. 5, pp. 1793–1800, Jun. 2005, doi: 10.1002/app.21619.

[33] A. K. Nikolaidis, D. S. Achilias, and G. P. Karayannidis, “Synthesis and characterization of PMMA/organomodified montmorillonite nanocomposites prepared by in situ bulk polymerization,” in *Industrial and Engineering Chemistry Research*, Jan. 2011, pp. 571–579. doi: 10.1021/ie100186a.

[34] S. Li, J. Qin, A. Fornara, M. Toprak, M. Muhammed, and D. K. Kim, “Synthesis and magnetic properties of bulk transparent PMMA/Fe-oxide nanocomposites,” *Nanotechnology*, vol. 20, no. 18, 2009, doi: 10.1088/0957-4484/20/18/185607.

[35] D. N. Uy Lan, S. Hadano, A. Abu Bakar, B. Azahari, Z. M. Ariff, and Y. Chujo, “Preparation of poly(methyl methacrylate) and polystyrene-composite-filled porous epoxy microparticles via in-situ suspension polymerization,” *Polym Test*, vol. 30, no. 8, pp. 841–847, Dec. 2011, doi: 10.1016/j.polymertesting.2011.08.002.

[36] M. Lahelin, M. Annala, A. Nykänen, J. Ruokolainen, and J. Seppälä, “In situ polymerized nanocomposites: Polystyrene/CNT and Poly(methyl methacrylate)/CNT composites,” *Compos Sci Technol*, vol. 71, no. 6, pp. 900–907, Apr. 2011, doi: 10.1016/j.compscitech.2011.02.005.

[37] G. Kim, S. Lim, B. H. Lee, S. E. Shim, and S. Choe, “Effect of homogeneity of methanol/water/monomer mixture on the mode of polymerization of MMA: Soap-free emulsion polymerization versus dispersion polymerization,” *Polymer (Guildf)*, vol. 51, no. 5, pp. 1197–1205, Mar. 2010, doi: 10.1016/j.polymer.2009.12.038.

[38] J. R. Street, A. L. Fricke, L. P. Reiss, A. L. Fricke, and L. P. Reiss, “Dynamics of Phase Growth in Viscous, Non-Newtonian Liquids: Initial Stages of Growth,” *Industrial and Engineering Chemistry Fundamentals*, vol. 10, no. 1, 1971, doi: 10.1021/i160037a011.

[39] D. F. Tirado and L. Calvo, “The Hansen theory to choose the best cosolvent for supercritical CO2 extraction of B-carotene from Dunaliella salina,” *Journal of Supercritical Fluids*, vol. 145, 2019, doi: 10.1016/j.supflu.2018.12.013.

[40] Martín-De León J and M. Ángel Rodríguez-Pérez, “TESIS DOCTORAL: UNDERSTANDING THE PRODUCTION PROCESS OF NANOCELLULAR POLYMERS BASED ON PMMA DRIVEN BY A HOMOGENEOUS NUCLEATION.”

[41] M. Ghasemi, A. Y. Singapati, M. Tsianou, and P. Alexandridis, “Dissolution of semicrystalline polymer fibers: Numerical modeling and parametric analysis,” *AIChE Journal*, vol. 63, no. 4, pp. 1368–1383, Apr. 2017, doi: 10.1002/aic.15615.

[42] J. Manjkow, J. S. Papanu, D. W. Hess, D. S. Soane, and A. T. Bell, “OXIDATION OF SILICON,” Aca-demic Press, 2003.

[43] J. Martín-De León, V. Bernardo, E. Laguna-Gutiérrez, and M. Ángel Rodríguez-Pérez, “Influence of the viscosity of poly(methyl methacrylate) on the cellular structure of nanocellular materials,” 2019, doi: 10.1002/pi.5920.

[44] S. Mane, S. Ponrathnam, and N. Chavan, “Synthesis and characterization of hypercrosslinked hydroxyl functionalized co-polymer beads,” *Eur Polym J*, vol. 59, 2014, doi: 10.1016/j.eurpolymj.2014.07.001.

6. APPENDIXES:

6.1. Appendix 1:

Polymerization is a key chemical process that combines monomers to form polymers. It plays a vital role in creating materials with tailored properties for various applications. The most used techniques are suspension, emulsion, and dispersion polymerization, with a preference for suspension polymerization [44]. These processes, known as free-radical polymerization, carried out by initiators and heat.

The phases of the polymerization process are:

- Initiation/Nucleation: This phase involves the activation of the polymerization reaction. It typically starts with the addition of an initiator, which generates free radicals or ions (**Fig. 22**). These initiators provide the necessary energy to initiate the polymerization process.

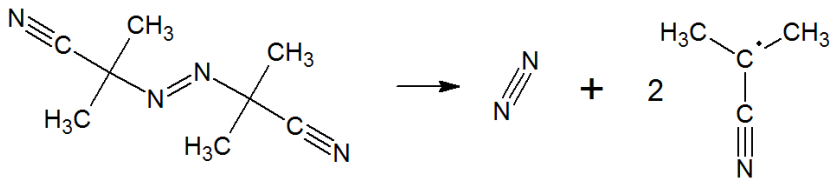

Fig. 22: *Decomposition of AIBN forming two 2-cyanopropyl free radicals with unpaired electrons.*

- Propagation: In this phase, the reactive species generated in the initiation phase react with monomers (**Fig. 23**), leading to the growth of polymer chains. The reactive species add monomer units one by one, extending the polymer chains and propagating the reaction.

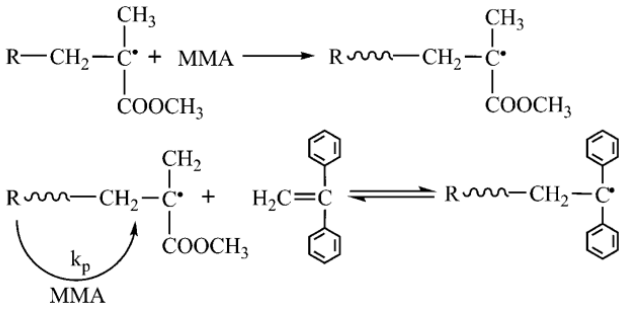

Fig. 23: *Free radical polymerisation of Methyl methacrylate (MMA) monomer to Poly Methyl methacrylate (PMMA) polymer with initiator (R).*

- Termination: Termination is the phase where the polymerization reaction comes to an end. It occurs when the reactive species, such as free radicals or ions, are consumed or deactivated. Termination can happen through various mechanisms, such as combination termination, where two growing polymer chains react with each other (**Fig. 24**), or disproportionation termination, where one chain transfers a hydrogen atom to another chain.

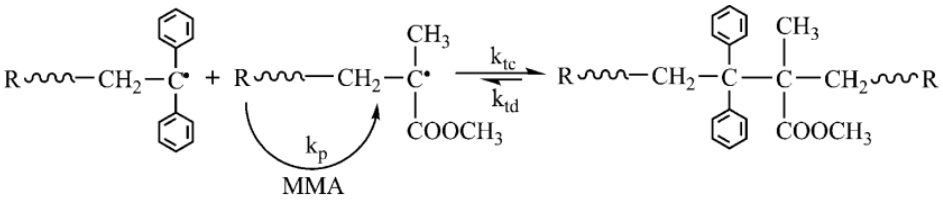

Fig. 24: *Chain termination of PMMA by combination of various smaller chains.*

- Chain transfer: Chain transfer is an additional phase that can occur in some polymerization reactions. It involves the transfer of a growing polymer chain to another molecule or species present in the reaction mixture. Chain transfer can affect the molecular weight and structure of the resulting polymer.

During polymerization, monomers act as building blocks for the polymer formation. Initiators are essential in starting the chain reaction by providing the necessary energy. They are reactive compounds that generate free radicals or ions to initiate polymerization.

The polymerization medium also influences the process. Bulk polymerization involves mixing monomers and initiators without a solvent, suitable for monomers that polymerize on their own or with activation. Solution polymerization dissolves monomers in a solvent, providing better control. Suspension and emulsion polymerizations disperse monomer droplets in a continuous phase, commonly water, using emulsifiers or stabilizers. These methods are ideal for insoluble monomers or when producing polymer particles. The choice of monomer and medium depends on desired properties and applications.

Chain termination occurs when polymer chains react, stopping further growth. Termination reactions include combination termination, where chains react to form a stable product, and disproportionation termination, where a chain transfers a hydrogen atom to another chain. Reaction conditions, such as temperature, pH, or reactant concentration, can also stop polymerization. Proper control of initiation and termination is crucial for desired polymer properties.

6.2. Used materials and discussion:

In every polymerization process a deoxygenated atmosphere with N_2 (g) is generated inside the flask. This is because nitrogen is an inert gas which does not react with any material used during polymerization. Air and most precisely O_2 (g) in it, can disturb the process, inhibiting the reaction if it reacts with free radicals or oxidizing functional groups. This technique is widely used in polymerization industry for achieving quality products free of impurities.

In bulk polymerization no other reactive is used apart from monomer and initiator. But in suspension and dispersion processes a medium is prepared using distilled deionized water (DDI H_2O), this is called the continuous phase. Also, polyvinyl alcohol (PVOH) is added due to its

hydrophilic and solubility in water properties. This reactive creates a thin layer around monomer particles preventing their agglomeration and maintaining their uniform dispersion in the aqueous medium. It also acts as adhesive and cohesive between polymer particles improving mechanical properties of the final product. Methanol (MeOH) is also used as solvent in reactions. It controls the velocity of the polymerization and stabilize it.

In this work MMA monomer is polymerizate it into PMMA. For starting the chain reaction, AIBN is used. It belongs to the group of organic compounds known as azo compounds, which contain a central azo (-N=N-) group. The election of this reactive is because it has a relatively low decomposition temperature (60-70°C) and because decomposition products are volatile and do not leave any significant residue. When heated, AIBN undergoes homolytic cleavage, generating two alkyl radicals, which can initiate the polymerization by reacting with monomers. On the other hand, potassium persulfate KPS is used instead of AIBN in emulsion polymerization, because it is soluble in DDI H_2O, the continuous phase. KPS is a free sulphate-radical ($SO_4^{\cdot -}$) initiator which abstract hydrogen atoms from MMA resulting in the formation of reactive polymer radicals. No MeOH is used in this free radical type of polymerization. Micelles are formed where KPS infiltrates and polymerization starts.

Stability and chain termination are important considerations to focus on when polymerize. Finishing the process in a clean and quick manner is important if the objective is to fabricate a monodisperse polymer. A reaction can be taken to an end reducing the temperature (thermal quenching), stopping the mechanical agitation (hindering monomer and initiator encounter), eliminating the initiator (or consumed it), neutralization (changing pH) or adding inhibitors.

The quantity of initiator, the duration of polymerization, the temperature, the agitation velocity, the solvent media, and the chosen process of polymerization affects to the molecular weight and polydispersity of the final polymer. Firstly, more proportion of initiator leads to lower molecular weights due to a higher density in starting points and shorter chains at the end of the process. This is exposed in M_n in Bulk_0.3 (141.800 g/mol) and in Bulk_0.04 (260.232 g/mol) samples [33], [34]. These methods where there is not an aqueous phase usually are characterized by a worst homogeneity mixing process because of an increment in viscosity. This tend to be reflected in higher PDI (4.0 and 3.7) than other methods.

Suspension_1 (115.290 g/mol) process was not as clear as Suspension (83.000 g/mol) because the agitation magnet was not big enough to mix the solution [35], [36]. This reflects on a higher molecular weight due to a poor interaction between initiator and monomer generating new chains. The use of MeOH in dispersion (63.750 g/mol) generates polymers with less M_w in comparison with suspension (83.800-115.290 g/mol) where is not used. This is explained due to interactions between the solvent and the initiator helping to a better dispersion and decomposition, once again

leading to the creation of new chains. The process of dispersion polymerization is divided into a particle nucleation stage and a particle growth stage. However, unlike other heterogeneous polymerizations, the particle nucleation stage occurs in a homogeneous phase. Due to the concentration rate of MeOH, polymerization take place by emulsion, but also by dispersion leading to a bimodal molecular weight distribution and high PDI (6.4) [38].

6.3. Appendix 2:

In this work pores that connect one cell to another have been measured with Fiji/Image J from SEM images (**Tab. 8**). Interconnected holes size is the mean value to control in filter and membrane manufacture. These materials show a huge range of sizes and densities. Also, porosity in percentage of open cell structure has been measured and exposed.

PMMA	ϕ_{in} (μm)	N_0 (nuclei/cm^3)	OC %
BULK_0.3	6.3±4.7	1.8E+07	98%
BULK_0.04	0.9±0.6	1.1E+09	82%
Suspension_1	0.5±0.4	4.9E+07	-
Emulsion	4.7±3.6	2.3E+09	98%
Suspension	2.1±1.9	4.9E+10	92%
Dispersion	16.6±3.6	5.3E+09	100%
VT	18.7±12.8	7.0E+06	86%

Tab. 8: *Inter connexions between cells sizes, their densities and open cell index.*

Pores sizes are in a range between 0.5±0.4 and 18.7±12.8 μm. Pores densities are in a range between 9.8E+06 μm and 4.9E+10 nuclei/cm^3. This creates a great variety of materials and a width tool to filter different particles sizes. Suspension density is so high due to its small size pore and because there is more than just one hole in most cells. Open cell percentage goes from 86-100%. The higher interconnected volume corresponds to Dispersion cellular material, the rest of the samples have also so high percentages.

Fig. 25 shows that in most of the cells from foamed samples there are at least one pore connecting this gas phase with another cell.

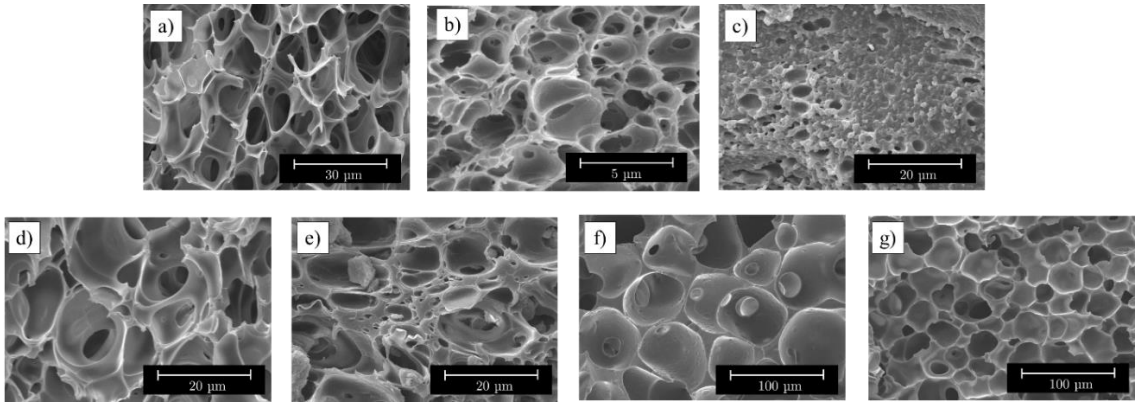

Fig. 25: *Detailed SEM images of different cellular structures and pores from: a) BulK_0.03. b) Bulk_0.04. c) Suspension_1. d) Emulsion. e) Suspension. f) Dispersion. g) VT.*

Fig. 26 shows a polynomic dependence between cell sizes and the pores that connect one with each other. Size distribution in these holes is high. So, pores are related with M_w and PDI in the same way cells are.

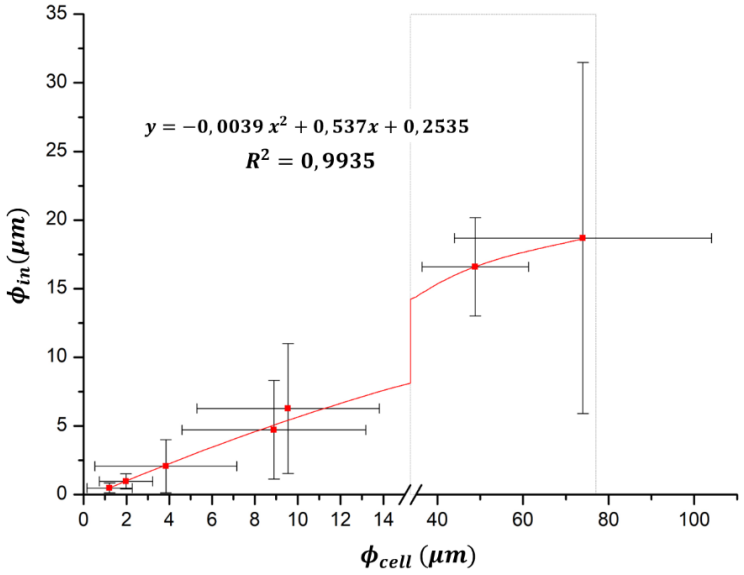

Fig. 26: Relation between cell size and pores that connect them.

Thanks to the use of cupcake filtering paper in the gas dissolution foaming process, a reduction in acetone evaporation is achieved before the gel is finally in the pressure vessel. Also results show that using this technique no macro size defects appear in samples, reduction and homogeneity in cell size also take place. The most important change is the exposition of cellular structure in external faces of the sample (**Fig. 27**). This characteristic of the production process opens the door to the use of this samples as membranes or filters without any other step or mechanical processing.

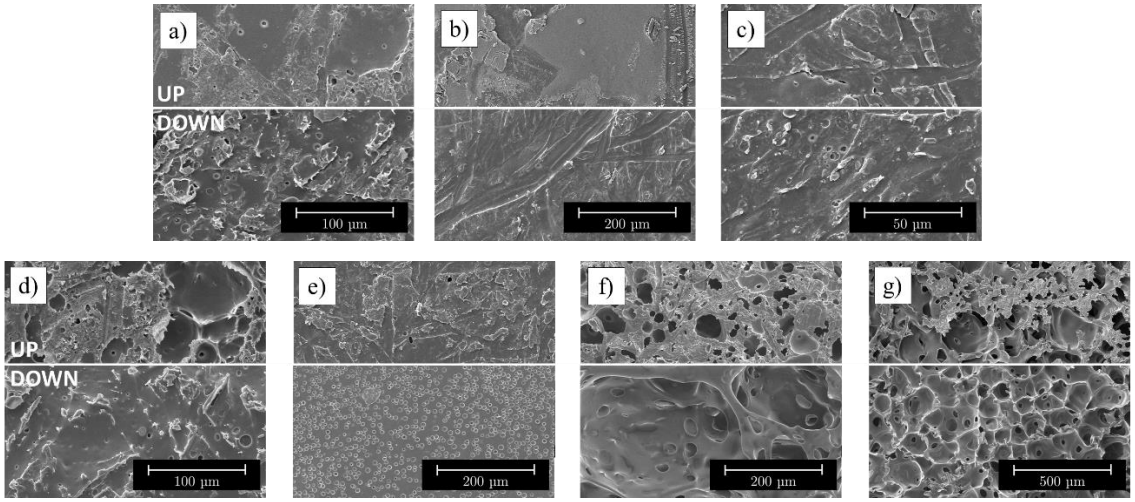

Fig. 27: Detailed SEM images from both faces of PMMA celllular materials: a) BulK_0.03. b) Bulk_0.04. c) Suspension_1. d) Emulsion. e) Suspension. f) Dispersion. g) VT.

As SEM images show, these exposed pores connect the outside with the inside structure of the sample. These allows mater to flow from one side to the other.

PMMA	ϕ_{up} (μm)	N_0 (pores/cm^3)	ϕ_{down} (μm)	N_0 (pores/cm^3)
BULK_0.3	1.9±1.3	1.8E+08	2.6±1.1	2.6E+08
BULK_0.04	-	-	-	-
Suspension_1	0.9±0.5	8.9E+06	1.3±1.1	1.3E+08
Emulsion	2.2±2.1	1.9E+08	1.8±1.5	6.8E+07
Suspension	8.0±4.6	5.0E+04	2.1±1.9	1.0E+07
Dispersion	12.3±9.5	1.9E+08	21.9±13.7	6.8E+07
VT	59.8±51.5	3.5E+06	43.2±34.4	7.9E+06

Tab. 9: *Pore sizes from both faces and their density nucleation.*

Pores sizes are in a range between 0.9±0.5 and 59.8.7±51.5 μm in the up face and 1.3±1.1 and 43.2±34.4μm in the down face. Pores densities are in a range between and 4.9E+10 nuclei/cm^3 in the up face and nuclei/cm^3 in the down face (**Tab. 9**).

Pores sizes in both faces and cells grow in the same manner (**Fig. 28**). So, pore size and nucleation density of these face holes could be explained by the same way cells have been with M_w and PDI. The only sample where no pores are generated in sample faces is Bulk_0.04. This event is well explained with the so high M_w of the polymer.

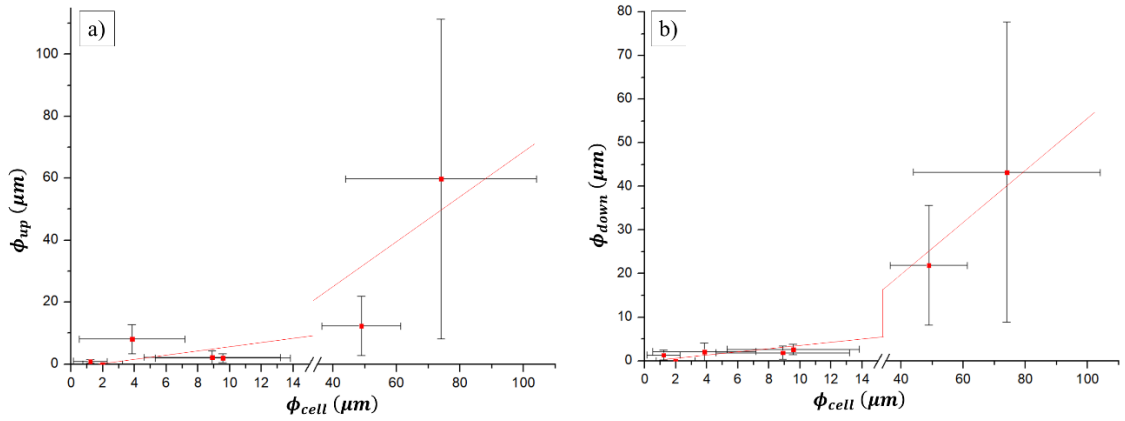

Fig. 28: *a) Cell size in relation to up face pores. b) Cell size in relation to down face pores.*